

## ORIGINAL ARTICLE

**Inhibition of tumor growth and metastasis *in vitro* and *in vivo* by targeting macrophage migration inhibitory factor in human neuroblastoma**Y Ren<sup>1,2</sup>, HM Chan<sup>1</sup>, J Fan<sup>3</sup>, Y Xie<sup>1</sup>, YX Chen<sup>1</sup>, W Li<sup>1</sup>, GP Jiang<sup>1</sup>, Q Liu<sup>1</sup>, A Meinhardt<sup>4</sup> and PKH Tam<sup>1</sup><sup>1</sup>Department of Surgery, The University of Hong Kong, Hong Kong, SAR, China; <sup>2</sup>Center for Hematology and Oncology Molecular Therapeutics, Taussig Cancer Center, Cleveland Clinic Foundation, Cleveland, OH, USA; <sup>3</sup>Statistics Laboratory, ORFE, Princeton University, Princeton, NJ, USA and <sup>4</sup>Department of Anatomy and Cell Biology, Justus-Liebig-University, Giessen, Germany

Macrophage migration inhibitory factor (MIF) has been defined as a novel oncogene. Our previous results have shown that MIF may contribute to the progression of neuroblastoma by (a) inducing N-Myc expression and (b) upregulating the expression of angiogenic factors. The aim of this study was to test whether tumor growth could be inhibited by reduction of endogenous MIF expression in neuroblastoma and clarify the molecular mechanisms underlying MIF reduction on the control of neuroblastoma growth. We established human neuroblastoma cell lines stably expressing antisense MIF (AS-MIF) cDNA. These stable transfectants were characterized by cell proliferation, gene expression profile, tumorigenicity and metastasis *in vitro* and *in vivo*. Decreased MIF expression was observed after transfection with AS-MIF in neuroblastoma cells and downregulation of MIF expression significantly correlated with decreased expression of N-Myc, Ras, c-Met and TrkB at protein level. Affymetrix microarray analysis revealed that expression of *IL-8* and *c-met* was inhibited and neuroblastoma-favorable genes such as *EPHB6* and *BLU* were upregulated in MIF reduced cells. Neuroblastoma cell growth exhibited a nearly 80% reduction in AS-MIF transfectants *in vitro*. Furthermore, mice in which tumors formed after subcutaneous injection of AS-MIF transfectants showed a 90% reduction in tumor growth compared to control. Metastasis in mice was also suppressed dramatically. Our data demonstrate that targeting MIF expression is a promising therapeutic strategy in human neuroblastoma therapy, and also identifies the MIF target genes for further study.

*Oncogene* (2006) 25, 3501–3508. doi:10.1038/sj.onc.1209395; published online 30 January 2006

**Keywords:** MIF; neuroblastoma; antisense; tumor growth and metastasis

Correspondence: Dr Y Ren, Center for Hematology and Oncology Molecular Therapeutics/R40, Taussig Cancer Center, Cleveland Clinic Foundation, Cleveland, OH 44195, USA.

E-mail: reny@ccf.org or

Professor P Tam, Department of Surgery, The University of Hong Kong Medical School, Hong Kong, SAR, China.

E-mail: paultam@hkucc.hku.hk

Received 22 August 2005; revised 13 December 2005; accepted 13 December 2005; published online 30 January 2006

**Introduction**

Neuroblastoma is one of the most common malignant tumors in children, and is responsible for about 15% of all pediatric cancer deaths (Maris and Matthay, 1999). Spontaneous regressions and differentiation *in vivo* are common in infants and in early-stage tumors, whereas children who are over 1 year of age at clinical presentation often have metastatic disease that fails to respond to medical intervention (Pritchard and Hickman, 1994). The underlying biological mechanism has not been fully elucidated. Despite recent advances in the management of the disease by conventional chemotherapy, the development of new therapeutic strategies is critically important.

The biological hallmark of neuroblastomas is the complexity of the genetic abnormalities acquired by the tumor cells. Some of these abnormalities are powerful prognostic markers that are independent of the clinical features. These genetic aberrations are ploidy changes, deletions of chromosome arms 1p and 11q, gains of chromosome arm 17q and amplification of the *N-myc* oncogene, (Bown, 2001). Overexpression of the N-MYC nuclear phosphoprotein is associated with advanced disease stage, rapid tumor progression and poor prognosis (Bown, 2001; Brodeur, 2003). Furthermore, expression of TrkB in human neuroblastoma is an important prognostic factor (Nakagawara *et al.*, 1993; Brodeur, 2003) and associated with N-Myc expression (Edsjo *et al.*, 2003). Despite intensive investigations, the fundamental role of these features in neuroblastoma initiation and progression remains obscure.

The effects of macrophage migration inhibitory factor (MIF) on the proinflammatory and immune responses have been known for some time, but it has also recently begun to be recognized as a protumorigenic factor (Mitchell and Bucala, 2000). Overexpression of MIF has been identified in prostatic lymph node metastases (Meyer-Siegler and Hudson, 1996), human melanomas (Shimizu *et al.*, 1999), breast carcinomas (Bini *et al.*, 1997), adenocarcinomas of the lung (Kamimura *et al.*, 2000), bladder cancer (Meyer-Siegler *et al.*, 2004) and hepatocellular carcinomas (Akbar *et al.*, 2001; Ren *et al.*, 2003a). It has been shown that high levels of MIF significantly correlate with an unfavorable outcome in

esophageal squamous cell carcinoma (Ren *et al.*, 2005) and hepatocellular carcinoma (Ren *et al.*, 2003a) and other tumors (del Vecchio *et al.*, 2000; Meyer-Siegler, 2000; Tomiyasu *et al.*, 2000). Our previous results revealed that MIF was highly expressed in neuroblastoma, and can stimulate oncogene *N-myc* expression and upregulate the expression of angiogenic factors (Ren *et al.*, 2004). MIF is also able to regulate the expression of genes related to tumor cell proliferation, migration and antiapoptosis (Fan *et al.*, 2004). These results suggest that MIF may play an important role in the development of neuroblastoma.

The aim of this study was to elucidate the mechanism of MIF in tumor development by investigating whether reduction of MIF expression could control tumor proliferation and tumorigenicity in neuroblastoma. We transfected neuroblastoma cells with antisense (AS)-MIF, and the properties of the AS-MIF-transfected clones were compared to those of control cells (transfected with empty vector).

## Results

### *MIF expression in cells transfected with AS-MIF vector*

Human neuroblastoma cell line SK-N-DZ, which expressed high level of MIF (Ren *et al.*, 2004), were transfected with control vector (vector alone) and AS-MIF vector. After hygromycin selection, 20 clones were picked, passaged and collected. MIF expression in these AS-MIF transfectants was further detected by Western blot analysis. Three representative clones named no. 3, no. 5 and no. 24 were used in this study. The result showed that the amount of MIF was substantially reduced in three clones compared to control cells (empty vector transfection; Figure 1).

### *Effects of AS-MIF transfection on expression of N-Myc, c-met, EPHB6 and other genes*

To better understand the molecular mechanism of MIF in the development of neuroblastoma, that is, whether MIF blockade can affect the production of molecules related to neuroblastoma development, Affymetrix

microarray and Western blot analysis were applied to identify genes or proteins whose expression was altered in AS-MIF-transfected cells. Western blot showed that AS-MIF transfection significantly inhibited N-Myc expression compared to control vector-transfected cells (Figure 1). Furthermore, Affymetrix microarray showed that of a total of about 22 283 probe sets, there were 44 genes changed in three clones transfected with AS-MIF more than twofold with *P*-value less than 0.001. The genes found to be up- or downregulated are selected in Table 1. The most interesting genes were *c-met*, *EPHB6*, Visinin-like protein-1 (*VSNL1*), *BLU*, *Ras* and interleukin-8 (*IL-8*). Table 1 showed that the average change of these genes was significantly different than in the control cells. The expression levels of *c-met*, *EPHB6*, *VSNL-1*, *Ras* and *BLU* were confirmed by real-time RT-PCR (Table 1). *IL-8* expression was confirmed by detection of *IL-8* in the supernatants of cell culture using enzyme-linked immunosorbent assay (ELISA) (Figure 2). In addition, Western blot analysis revealed that expression of TrkB, c-Met and Ras was markedly inhibited in clone no. 3, no. 5 and no. 24 compared to cells transfected with vector alone (Figure 3). The phosphorylation of TrkB and c-Met was also reduced in these clones (Figure 3).

Affymetrix microarray and real-time RT-PCR data showed that oncogene *c-met* mRNA was suppressed in

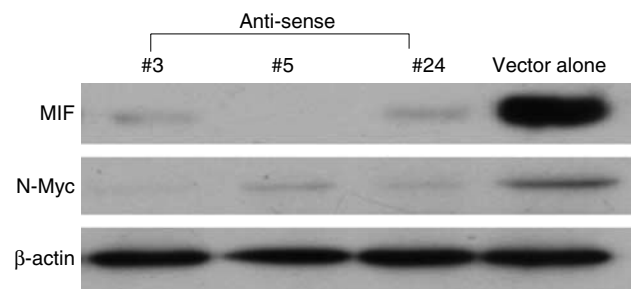


**Figure 1** The expression of MIF and N-Myc in human neuroblastoma cell line SK-N-DZ transfected with AS-MIF (clone no. 3, no. 5 and no. 24) and vector alone. MIF and N-Myc were detected by Western blot. Suppression of MIF expression was observed in neuroblastoma cells transfected with AS-MIF (clone no. 3, no. 5 and no. 24) compared with cells transfected with vector alone, as was the downregulation of the expression of N-Myc.

**Table 1** Genes identified by Affymetrix analysis and confirmed by real-time quantitative PCR or ELISA

GeneBank	Description	Fold change	P-value <sup>a</sup>	RT-PCR confirmation (fold change)
NM_005651	Tryptophan 2,3-dioxygenase (TDO2)	-3.15 ± 0.16	0.0000	-5.16 ± 0.18*
NM_000584	Interleukin 8 (IL-8) <sup>b</sup>	-13.22 ± 0.40	0.0000	
M33653	α2 type IV collagen (COL4A2)	4.27 ± 0.28	0.0000	9.38 ± 0.45*
AF039555	Visinin-like protein-1 (VSNL-1)	1.58 ± 0.08	0.0007	4.89 ± 0.38*
NM_004445	EPHB6	2.64 ± 0.22	0.0022	12.38 ± 0.33*
NM_006509	Reticuloendotheliosis viral oncogene homolog B	-1.91 ± 0.16	0.0043	-3.61 ± 0.49*
NM_004369	Collagen type VI, α3 (COL6A3)	2.37 ± 0.23	0.0160	10.34 ± 0.44*
NM_004464	Fibroblast growth factor 5 (FGF5)	-1.46 ± 0.11	0.0259	-1.95 ± 0.36*
BE870509	Met proto-oncogene <sup>c</sup>	-1.58 ± 0.14	0.0338	-1.85 ± 0.16*
AC002481	BLU	1.79 ± 0.20	0.0799	1.66 ± 0.24*
NM_004578	RAS oncogene family (RAB4) <sup>c</sup>	-1.36 ± 0.12	0.1710	-2.37 ± 0.27*

ELISA = enzyme-linked immunosorbent assay; PCR = polymerase chain reaction; RT = reverse transcriptase. \*Significantly different from control (*P* < 0.05). <sup>a</sup>Multiplied by 100. <sup>b</sup>Confirmed by ELISA. <sup>c</sup>Confirmed by Western Blot.

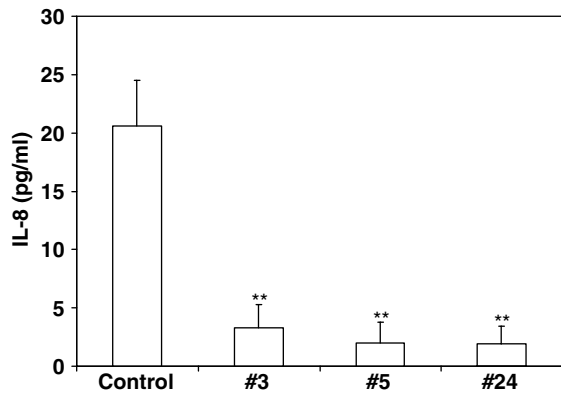


**Figure 2** ELISA measurement of IL-8 in cell supernatants of AS-MIF transfectants. Cells in 24-well plates at  $3 \times 10^5$  were cultured with DMEM with 10% FBS for 24 h. The culture supernatants were collected and IL-8 were measured by ELISA (mean  $\pm$  s.d.,  $n = 5$ , \*\* $P < 0.001$ ).

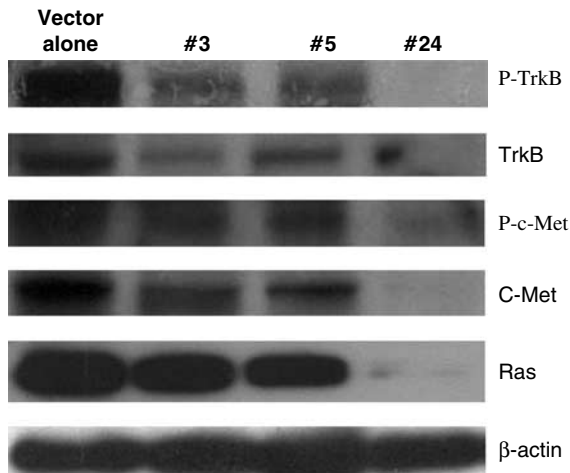


**Figure 3** The expression of c-Met, TrkB and Ras in AS-MIF transfectants (no. 3, no. 5 and no. 24) and vector alone detected by Western blot. The expression c-Met, TrkB and Ras, and the activation of c-Met and TrkB were suppressed in neuroblastoma cells transfected with AS-MIF (clone no. 3, no. 5 and no. 24) compared with cells transfected with vector alone.

AS-MIF-transfected cells (Table 1). We therefore further studied the association of MIF and c-Met in neuroblastoma specimens from patients by immunohistochemical staining. MIF expression was found in all specimens of neuroblastoma ( $n = 21$ ). The expression of MIF and c-Met was seen in the cytoplasm of tumor cells in all cases. Double immunohistochemical staining showed that neuroblastoma cells expressed MIF and c-Met protein strongly (Figure 4). Furthermore, there was a significant positive correlation between expression of MIF and c-Met ( $r = 0.635$ ,  $P = 0.002$ ).

#### Effect of AS-MIF on cell growth in vitro

To detect whether the reduction of MIF expression affects neuroblastoma cell growth *in vitro*, cells were cultured in Dulbecco's minimum essential medium

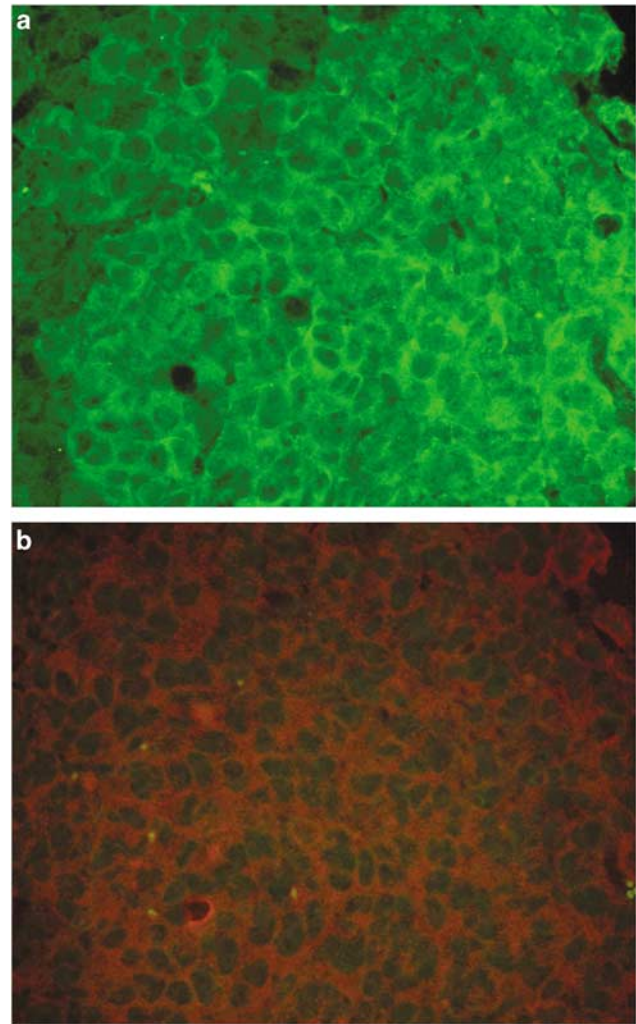


**Figure 4** Expression of MIF and c-Met in neuroblastoma analysed by double immunohistochemical staining (original magnification,  $\times 20$ ). c-Met and MIF are stained green and red, respectively. The majority of neuroblastoma cells express c-Met throughout the cytoplasm (a) and MIF (b).

(DMEM) with 10% fetal bovine serum (FBS) for 3 days, and proliferation was determined by 3-(4,5-dimethylthiazol-2-yl)-2,5-diphenyltetrazolium bromide (MTT) assay. As shown in Figure 5, the proliferation rates of clone no. 3, no. 5 and no. 24 were suppressed significantly to 60.3, 52.5 and 78.4%, respectively, compared with those of the cells transfected with vector alone.

#### Effect of AS-MIF on cell apoptosis

To detect whether the reduction of MIF expression can induce neuroblastoma cell apoptosis, cells were cultured in DMEM with 2% FBS for 48 h and the spontaneous apoptosis was detected by Annexin V binding assay. As shown in Figure 6, numbers of cells from clone no. 3, no. 5 and no. 24 that were undergoing spontaneous apoptosis were significantly higher compared to cells transfected with vector alone.

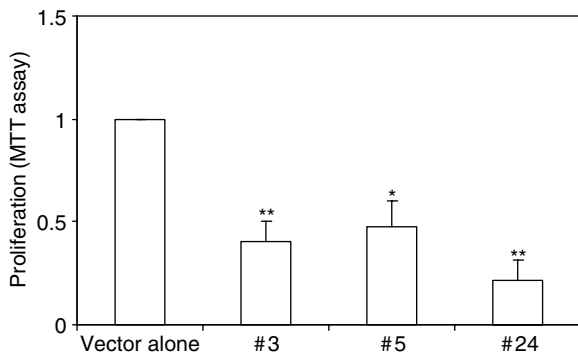


**Figure 5** Effect of AS-MIF transfection on neuroblastoma cell proliferation. Cells ( $1 \times 10^4$ ) were cultured in 96-well plate for 72 h. Cell proliferation was examined by MTT colorimetric assay. AS-MIF transfection resulted in a decrease in cell proliferation. Values represent the mean of three experiments conducted in triplicate and are expressed as mean  $\pm$  s.d. (\* $P < 0.05$ , \*\* $P < 0.001$ ).

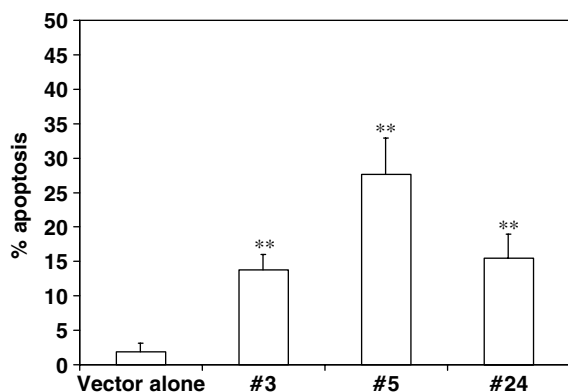


**Figure 6** Effect of AS-MIF transfection on neuroblastoma cell apoptosis. Apoptosis was determined by Annexin V binding, as compared with control cells. All of the results were expressed as the mean of three independent experiments  $\pm$  s.d. (\*\* $P < 0.001$ ).

#### Effect of AS-MIF on cell invasiveness in vitro

The invasiveness of AS-MIF transfectants was evaluated using an *in vitro* invasion assay. We found that cell numbers of clone no. 3, no. 5 and no. 24 that penetrated the Matrigel were significantly reduced to those of neuroblastoma cells transfected with vector alone ( $P < 0.001$ ; Figure 7).

#### Effects of AS-MIF transfection on tumor growth and metastasis in vivo

Given these findings *in vitro*, we further analysed the effect of suppressing MIF expression on tumor growth and metastasis in athymic nude mice. For a tumor growth mouse xenograft model, mice were inoculated subcutaneously with  $1 \times 10^6$  cells. Empty vector-transfected neuroblastoma cells formed progressively, growing solid tumors in all mice ( $n = 10$ ; Figure 8). By contrast, clone no. 3, no. 5 and no. 24 produced much smaller tumors ( $n = 10$  for each clone; Figure 8). We further investigated the metastatic potential of AS-MIF transfectants. Nude mice were injected intravenously with  $2 \times 10^6$  neuroblastoma cells transfected with vector alone or clone no. 3, no. 5 and no. 25 ( $n = 10$  for each

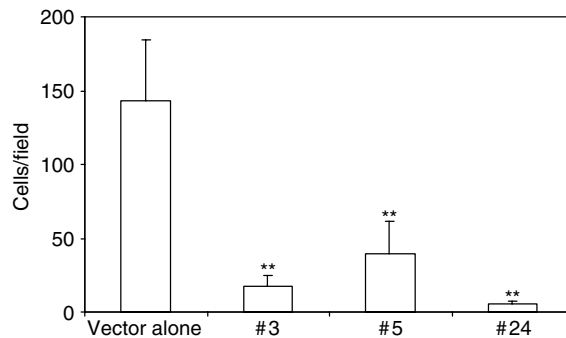


**Figure 7** Effect of AS-MIF transfection on neuroblastoma cell migration. AS-MIF transfection significantly suppressed neuroblastoma cell migration. Values represent the mean of three experiments conducted in triplicate and are expressed as mean  $\pm$  s.d. (\*\* $P < 0.001$ ).

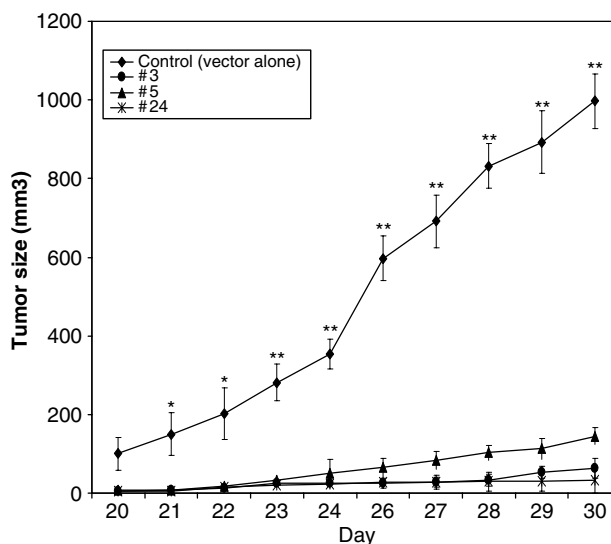


**Figure 8** Neuroblastoma growth curve of AS-MIF transfectants in nude mice. Nude mice were injected subcutaneously with cells transfected with AS-MIF or vector alone. Tumor development was followed to 1 month. Tumor growth was retarded almost completely in AS-MIF transfectants no. 3, no. 5 and no. 24, in contrast to control cells. Values are means  $\pm$  s.d. ( $n = 10$ ; \* $P < 0.05$ , \*\* $P < 0.001$ ).

clone and control). After 2–3 months of the injection, 70% mice in control group developed lung metastasis (Figure 9a), whereas only 10–20% mice developed lung metastasis in AS-MIF-transfected groups (Table 2). Histological examination indicated tumor cells in the lung (Figure 9b).

#### Effects of AS-MIF transfection on formation of capillary vessels

Angiogenesis is required for the growth, expansion and metastasis of tumors. We therefore observed the angiogenesis of tumors derived from the AS-MIF transfectants ( $n = 10$  for each clone) and cells transfected with vector alone ( $n = 10$ ). The tumors derived from AS-MIF transfectants had a lower microvessel density (MVD) than those from the control cells. The tumor MVD in tumors derived from AS-MIF group ( $n = 30$ ) was  $12.3 \pm 1.5$ /high-power field (HPF) and  $47.9 \pm 4.8$ /HPF of the control cells ( $n = 10$ ).

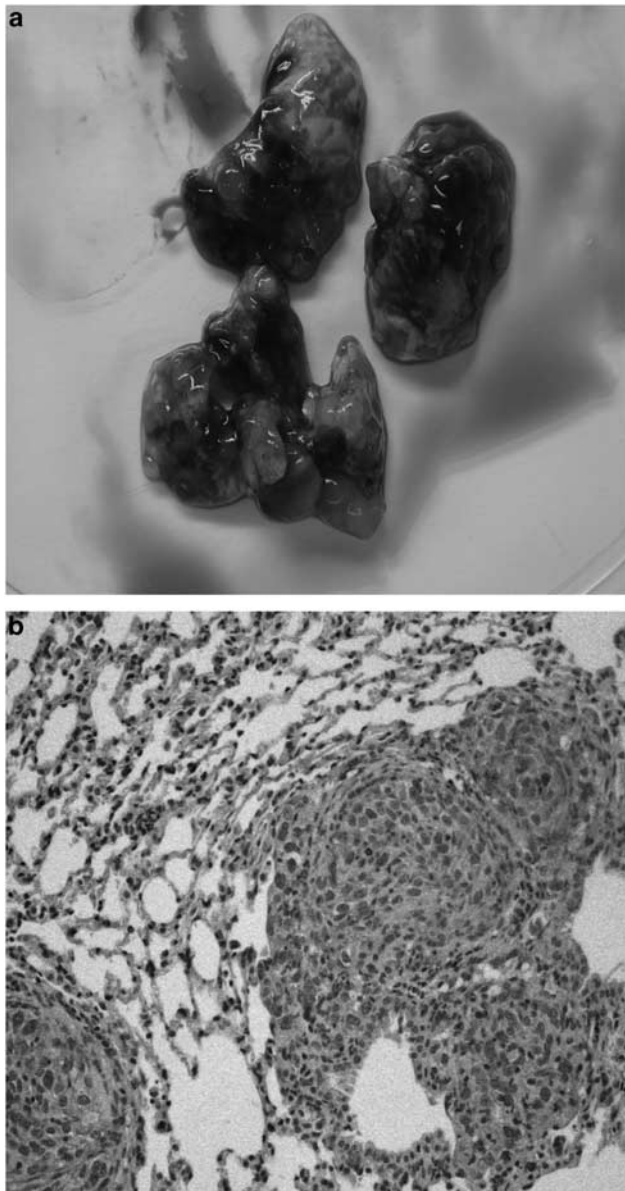


**Figure 9** Lung metastatic tumor growth in nude mice. The representative metastatic neuroblastoma in lung (a) and H&E staining image of tumor (b).

**Table 2** AS-MIF transfection inhibits neuroblastoma metastasis *in vivo*

	Liver metastasis	Lung metastasis
No. 3	1/10	1/10
No. 5	2/10	1/10
No. 24	1/10	2/10
Control	6/10*	7/10*

AS-MIF = antisense MIF. \* $P < 0.05$ .

## Discussion

Overexpression of MIF is frequently observed in a number of different primary carcinomas. However, little is known about the functional role of MIF in the pathogenesis and progression of neuroblastoma. Our

previous research has shown that human neuroblastoma expresses high levels of MIF, and the overexpression of MIF significantly correlates with tumor grade and N-Myc expression (Ren *et al.*, 2004). To assay a possible functional relationship between MIF expression and tumorigenicity in neuroblastoma, SK-N-DZ neuroblastoma cells were transfected with an AS-MIF expression vector, and a decrease in MIF expression in neuroblastoma cells was observed after transfection. Our data revealed that c-Met, N-Myc, TrkB, Ras and IL-8 were inhibited and neuroblastoma favorable genes such as *EPHB6* and *BLU* were upregulated in MIF reduced cells. We demonstrated that downregulation of MIF expression can result in a reduction in cell proliferation and tumor growth and metastasis *in vitro* and in nude mice.

It has been reported that MIF is able to enhance tumor cell growth (Nishihira *et al.*, 2003). Several studies have also shown that reduction of MIF results in the inhibition of tumor cell proliferation in bladder cancer (Meyer-Siegler *et al.*, 2004), melanoma (Shimizu *et al.*, 1999) and colon cancer (Sasaki *et al.*, 2002). However, the molecular mechanisms are poorly understood. We have previously demonstrated that MIF was highly expressed in neuroblastoma cells and that its expression is significantly correlated with cell differentiation, suggesting the involvement of MIF in neuroblastoma cell proliferation and differentiation. Consistent with these findings, we have now established that AS-MIF transfection markedly suppresses neuroblastoma growth and metastasis *in vitro* and *in vivo*. We further investigated the possible mechanism for this phenomenon. We first showed that expression of N-Myc, c-Met, TrkB, Ras and IL-8 levels were decreased, and *EPHB6* and *BLU* levels increased, in AS-MIF transfectants. It has been shown that *N-myc* amplification is associated with advanced disease stage, rapid tumor progression and poor prognosis in neuroblastoma (Seeger *et al.*, 1988, 1985). *N-myc* is associated with tumorigenesis and cell proliferation (Chambery *et al.*, 1999). In our previous study, we observed that MIF could stimulate expression of both *N-myc* mRNA and N-Myc protein in neuroblastoma cells (Ren *et al.*, 2004). *C-met* has been identified as an activated oncogene (Park *et al.*, 1986). A large number of studies have shown that c-Met is frequently expressed in carcinomas and in other types of human solid tumors and their metastases. Overexpression of c-Met is often associated with poor prognosis (Birchmeier *et al.*, 2003). Highly invasive neuroblastoma cells express c-Met and the presence of paracrine HGF/c-met signaling was associated with increased neuroblastoma invasiveness *in vitro* and *in vivo* (Hecht *et al.*, 2004). The recent study showed that TrkB cooperated with c-Met-enhanced neuroblastoma invasiveness (Hecht *et al.*, 2005). In the present study, our data showed that the expression of c-Met and TrkB was decreased in MIF reduced cells and MIF expression significantly correlated with c-Met protein expression in human neuroblastoma specimens. This strongly indicates that MIF may have a function in upregulating c-Met or TrkB expression. *EPHB6* is a favorable neuroblastoma gene, which is downregulated

in the most aggressive neuroblastoma cell lines. It is a prognostic indicator in neuroblastoma and other tumors such as melanoma and breast cancer (Tang *et al.*, 2000, 2004; Hafner *et al.*, 2003; Fox and Kandpal, 2004). High-level expression of *EPHB6* predicts favorable neuroblastoma outcome, and forced expression of these genes inhibits growth of unfavorable neuroblastoma cells (Tang *et al.*, 2000). However, it is not clear how *EPHB6* is regulated. A particularly significant finding of this study was that *EPHB6* was increased in MIF reduced neuroblastoma cells. This result suggests a promising direction for the further study of the relationship between MIF and *EPHB6*. *VSNL-1* is expressed in the central nervous system, where it plays a crucial role in regulating cAMP levels, cell signaling and differentiation. High-level *VSNL-1* expression is also associated with less aggressive and high-grade squamous cell carcinoma (Mahloogi *et al.*, 2003). This indicates that *VSNL-1* may play an important role in regulating tumor cell invasiveness, and that its loss could aid in enhancing the advanced malignant phenotype. *BLU* is abundantly expressed in normal lung tissue. However, its expression is drastically reduced in a subset of lung tumor cell lines (Agathangelou *et al.*, 2003). *BLU* is also inactivated in neuroblastoma. Methylation of the *BLU* promoter region (inactivation of *BLU*) in neuroblastoma inversely correlates with tumor stage (Agathangelou *et al.*, 2003). These data suggest that *BLU* is one of the candidate tumor suppressor genes. Taken together, we found a number of genes or proteins whose expression levels were markedly modified by MIF. We suggest that these genes may be involved in the MIF-induced tumor growth inhibition.

Angiogenesis is a critical process in the development and metastasis of many solid tumors, including neuroblastoma. It has been reported that the vascularity of neuroblastoma in patients with widely metastatic disease is significantly higher than that in patients with local or regional disease, and that vascularity shows a strong inverse correlation with the survival of patients (Meitar *et al.*, 1996). One of the important activities of MIF in promoting tumorigenesis and metastasis is to stimulate angiogenesis (Ogawa *et al.*, 2000). Recent studies have shown that immunoneutralization of MIF during the initial stage of lymphoma growth has profound effects on tumor size (Chesney *et al.*, 1999), and that MIF is a required factor for tumor-initiated endothelial cell proliferation (Yang *et al.*, 2000). This indicates that MIF may function to stimulate tumor-associated angiogenesis by a direct effect on endothelial growth. However, the role of MIF in angiogenesis involving tumor and endothelial cells is less well understood. IL-8 has been identified as an angiogenesis-regulating molecule that induces angiogenesis (Koch *et al.*, 1992; Desbaillets *et al.*, 1997). The expression of IL-8 has been found in various human cancers (Xie, 2001). Recent studies have also demonstrated that IL-8 regulates tumor cell growth and metastasis in many tumors such as melanoma, carcinoma of breast, stomach, pancreas and liver. Our previous results indicated that serum IL-8 from patients with hepatocellular carcinoma significantly correlated with tumor size,

tumor stage and venous invasion (Ren *et al.*, 2003b), suggesting that IL-8 may be directly or indirectly involved in tumor progression. We have also demonstrated that MIF is able to stimulate neuroblastoma cells to express IL-8 (Ren *et al.*, 2004). This study has demonstrated that IL-8 gene expression is drastically decreased in MIF reduced cells (>13-fold), and an ELISA assay has confirmed that the volume of IL-8 protein produced by MIF reduced cells was 10 times lower than in the control cells. In addition, amplification of *N-myc* is associated with enhanced angiogenesis of human neuroblastoma (Meitar *et al.*, 1996). It has recently been reported that enhanced expression of *N-myc* in human neuroblastoma cells downregulates an inhibitor of endothelial cell proliferation, activin A. We have shown in this study that MVD in tumors derived from AS-MIF transfectants was significantly lower than in the control tumors. Overall, the study's findings provide evidence that AS-MIF treatment may exert its antiangiogenic effects via suppression of IL-8 and *N-Myc*.

In conclusion, we have demonstrated that blocking MIF expression would benefit tumor control in neuroblastoma by inhibiting tumor growth, angiogenesis and metastasis. With this approach, we have shown that reduction of MIF results in tumor growth inhibition, and that suppression may be achieved by inhibiting *N-Myc*, IL-8, *c-Met* and *TrkB*. On the other hand, increasing the expression of tumor suppressor genes (*BLU*, *VSNL-1*) and neuroblastoma favorite gene (*EPHB6*) may also contribute to tumor reduction. Therefore, these genes could potentially be key players in the development of neuroblastoma. Our data not only demonstrate that targeting MIF expression is a promising therapeutic strategy for human neuroblastoma therapy but also identify the MIF target genes for further study.

## Materials and methods

### Cells

Human neuroblastoma cell line SK-N-DZ was obtained from American Type Culture Collection (ATCC; Rockville, MD, USA). Cells were maintained in DMEM supplemented with 10% FBS (Gibco BRL-life Technologies, Grand Island, NY, USA) and 1% penicillin–streptomycin in a humidified incubator (95% air and 5% CO<sub>2</sub>) at 37°C.

### Tissue samples

Tumor specimens were obtained from 21 patients with surgically resected primary neuroblastoma treated between 1990 and 2000 in Queen Mary Hospital, Hong Kong. The patients included 16 males and five females, and their median age at diagnosis was 60 months (range: 6.0–240 months). Representative blocks from both tumorous and non-tumorous tissues from each specimen were taken for immunohistochemical study.

### Construction of expression vectors and transfection of neuroblastoma cells

An MIF AS expression plasmid was constructed by cloning human MIF cDNA corresponding to nucleotides 98–445

(GeneBank Accession No. NM-002415) with *HindIII* and *XhoI* adaptors in 3'-5' orientation into pCMV-containing expression vector pSecTag2/Hygro (Invitrogen Corp., Carlsbad, CA, USA). The pSec/AS MIF expression vector or the parental (control) pSec vector was transfected into neuroblastoma cell line SK-N-DZ with Lipofectamine 2000 (Invitrogen), and stable clones were selected by resistance to hygromycin (300 µg/ml; Geneticin-Life Technologies, Gaithersburg, MD, USA) and expanded into cell lines. Three clones (no. 3, no. 5 and no. 24) transfected with MIF AS-expressing vectors were analysed for MIF expression by Western blot. All three clones showed low levels of MIF expression (Figure 1). The cells transfected with empty vector were used as a control.

#### RNA isolation and application to Affymetrix GeneChip

Total RNA samples were prepared from cell culture with the TRIzol reagent (Invitrogen) according to the manufacturer's directions. Probe synthesis and hybridization of human U-133A GeneChip Oligo Microarrays (Affymetrix, Santa Clara, CA, USA) were performed in accordance with the manufacturer's instructions. Gene expression data (CHP file of Affymetrix Microarray Suite 5.0 software) were normalized to a global target intensity of 500.

#### Real-time quantitative RT-PCR

Total RNA (0.5 µg) was used to generate cDNA using the Taqman Reverse Reagents (Applied Biosystems, Foster City, CA, USA). Taqman Universal PCR Master Mix and Taqman Gene Expression Assays, which contain the primers for candidate genes (*TDO2*, *FGF5*, *Met*, *VSNL-1*, *EPHB6*, *COL6A3*, *Intergrin* and *Blu*; Applied Biosystems, Foster City, California), were performed for detecting RT-PCR products. Pre-normalized primers for 18S ribosomal RNA were obtained from Applied Biosystems (Foster City, CA, USA). The PCR cycling conditions were performed for all of the samples, as follows: 2 min at 50°C for incubation; 10 min at 95°C for AmpliTaq amplification and 40 cycles for the melting (95°C for 15 s) and annealing/extension (60°C for 1 min) steps. PCR reactions for each template were performed in triplicate in one 96-well dish per gene-specific primer pair tested. The comparative  $C_T$  method (Livak and Schmittgen, 2001) was used to quantitate the expression for each gene.

#### Western blot analysis

Cells were washed with phosphate-buffered saline (PBS), and directly lysed in RIPA buffer (0.5% sodium deoxycholate, 0.1% sodium dodecyl sulfate (SDS), 1% NP-40 and PBS) with PMSF and proteases inhibitors. Protein concentration was determined by Bio-Rad DC assay (Bio-Rad, Hercules, CA, USA). The samples were adjusted to equal protein concentrations and subjected to SDS-polyacrylamide gel electrophoresis (SDS-PAGE). Proteins on the gel were transferred onto nitrocellulose membranes blocked with 5% bovine serum albumin in Tris-buffered saline containing 0.1% Tween-20 for 1 h at room temperature. The membranes were then incubated with the indicated primary antibodies overnight at 4°C, washed with PBS and incubated with the appropriate secondary antibody. The immunoreactive bands were visualized with chemiluminescence (ECL, Amersham, UK).

#### Double immunohistochemical staining

Paraffin sections were incubated with primary c-Met monoclonal antibody (mAb) overnight at 4°C. Sections were then washed with PBS (pH 7.4). Endogenous peroxidase was inactivated with 3% H<sub>2</sub>O<sub>2</sub> in methanol, and then incubated

with goat anti-mouse IgG-FITC (Sigma, St Louis, MO, USA) for 2 h at room temperature. Sections were then mounted with medium for fluorescence with DAPI (Vector Laboratories, Burlingame, CA, USA). Electronic images of the immunofluorescence visualized under a fluorescence microscope (Nikon eclipse E600, Japan) were saved to PC. The sections were then washed with PBS. After microwave heating, antibody against MIF was applied as primary antibody at 4°C overnight on same sections, and sections were then incubated with anti-mouse universal immunoalkalinephosphatase polymer (Nichirei Corporation, Tokyo, Japan) for 2 h at room temperature. The color was subsequently developed with fast red substrate system (Sigma). Sections were mounted with same mounting medium above. The same fields as in the immunofluorescence images were subsequently selected and visualized under the same microscope and also saved as electronic images for comparison and analysis of colocalization.

#### Cell proliferation assay

Cells ( $1 \times 10^4$ ) were placed in each well of a 96-well plate and cultured in DMEM with 10% FBS for 72 h. The cell proliferation was examined by MTT colorimetric assay in the formazan product and MTT was measured as absorbance at 550 and 650 nm.

#### Apoptosis assay

Cells were cultured in six-well plate in DMEM with 2% FBS for 48 h, and then stained with FITC-conjugated anti-Annexin-V antibody (Boehringer Mannheim, Mannheim, Germany). Labeled cells were assayed by a FACScan flow cytometer (Becton Dickinson, Mountain View, CA, USA) that automatically and simultaneously measured the fluorescence of individual cells identified by their size-dependent light-scattering properties.

#### In vitro invasion assay

Tumor cell invasion and migration were assayed in the invasion chamber (Becton Dickinson Labware) with 8 µm-porosity polycarbonate filter membrane. The upper sides of the membranes were precoated with Matrigel matrix (Becton Dickinson Labware; 30 µg/insert). The coated insert was placed in each well of a 24-well plate filled with 500 µl of medium (MEM with 1% FCS). The upper well contained tumor cell suspension (200 µl,  $1 \times 10^4$  cell/ml medium). The cells in the chambers were incubated for 24 h at 37°C, and migration to the underside of the pre-coated filter was measured. For each chamber, the number of migrated cells in five randomly chosen high-power fields was counted.

#### Tumor growth in nude mice

The 6-week-old BALB/c nude mice (Laboratory Animal Unit, The University of Hong Kong, Hong Kong, SAR, China) were injected subcutaneously with  $2 \times 10^6$  SK-N-DZ transfected with vector alone (control cell line,  $n=10$ ) or AS-MIF-transfected cells lines (no. 3, no. 5 and no. 24;  $n=10$  for each cell line). Tumor growth in each group was monitored everyday by two-dimensional measurements of individual tumors from each mouse.

#### Tumor metastasis in nude mice

The 6-week-old BALB/c nude mice were injected intravenously with  $2 \times 10^6$  SK-N-DZ transfected with vector alone or AS-MIF-transfected cells ( $n=10$ ). All mice were monitored on a weekly basis for bodyweight and other abnormalities. Once

life-threatening symptoms became markedly manifest, the mouse was killed by cervical dislocation. The tumors in the lungs were excised and fixed with 4% formalin for H&E staining.

#### Evaluation of MVD

Tissue sections were immunostained with human CD34 mAb and scanned by light microscopy at low-power field ( $\times 40$ ) and the vessel count in areas with the highest number of capillaries was assessed at HPF ( $\times 200$ ). The average counts of five fields were determined. The MVD was counted by two neutral investigators without specialized knowledge of MIF and neuroblastoma.

#### References

- Agathangelou A, Dallol A, Zochbauer-Muller S, Morrissey C, Honorio S, Hesson L *et al.* (2003). *Oncogene* **22**: 1580–1588.
- Akbar SM, Abe M, Murakami H, Tanimoto K, Kumagi T, Yamashita Y *et al.* (2001). *Cancer Lett* **171**: 125–132.
- Bini L, Magi B, Marzocchi B, Arcuri B, Tripodi S, Cintorino M *et al.* (1997). *Electrophoresis* **18**: 2832–2841.
- Birchmeier C, Birchmeier W, Gherardi E, Vande Woude GF. (2003). *Nat Rev Mol Cell Biol* **4**: 915–925.
- Bown N. (2001). *J Clin Pathol* **54**: 897–910.
- Brodeur GM. (2003). *Nat Rev Cancer* **3**: 203–216.
- Chambery D, Mohseni-Zadeh S, de Galle B, Babajko S. (1999). *Cancer Res* **59**: 2898–2902.
- Chesney J, Metz C, Bacher M, Peng T, Meinhardt A, Bucala R. (1999). *Mol Med* **5**: 181–191.
- del Vecchio MT, Tripodi SA, Arcuri F, Pergola L, Hako L, Vatti R *et al.* (2000). *Prostate* **45**: 51–57.
- Desbaillets I, Diserens AC, Tribolet N, Hamou MF, Van Meir EG. (1997). *J Exp Med* **186**: 1201–1212.
- Edsjo A, Nilsson H, Vandesompele J, Karlsson J, Pattyn F, Culp LA *et al.* (2003). *Lab Invest* **83**: 813–823.
- Fan J, Tam P, Vande Woude G, Ren Y. (2004). *Proc Natl Acad Sci USA* **101**: 1135–1140.
- Fox BP, Kandpal RP. (2004). *Biochem Biophys Res Commun* **318**: 882–892.
- Hafner C, Bataille F, Meyer S, Becker B, Roesch A, Landthaler M *et al.* (2003). *Int J Oncol* **23**: 1553–1559.
- Hecht M, Papoutsi M, Tran HD, Wilting J, Schweigerer L. (2004). *Cancer Res* **64**: 6109–6118.
- Hecht M, Schulte JH, Eggert A, Wilting J, Schweigerer L. (2005). *Carcinogenesis* **26**: 2105–2115.
- Kamimura A, Kamachi M, Nishihira J, Ogura S, Isobe H, Dosaka-Akita H *et al.* (2000). *Cancer* **89**: 334–341.
- Koch AE, Polverini PJ, Kunkel SL, Harlow LA, DiPietro LA, Elnor VM *et al.* (1992). *Science* **258**: 1798–1801.
- Livak KJ, Schmittgen TD. (2001). *Methods* **25**: 402–408.
- Mahloogi H, Gonzalez-Guerrico AM, Lopez De Cicco R, Bassi DE, Goodrow T, Braunewell KH *et al.* (2003). *Cancer Res* **63**: 4997–5004.
- Maris JM, Matthay KK. (1999). *J Clin Oncol* **17**: 2264–2279.
- Meitar D, Crawford SE, Rademaker AW, Cohn SL. (1996). *J Clin Oncol* **14**: 405–414.
- Meyer-Siegler K. (2000). *J Interferon Cytokine Res* **20**: 769–778.
- Meyer-Siegler K, Hudson PB. (1996). *Urology* **48**: 448–452.
- Meyer-Siegler KL, Leifheit EC, Vera PL. (2004). *BMC Cancer* **4**: 4:34.
- Mitchell RA, Bucala R. (2000). *Semi Cancer Biol* **10**: 359–366.
- Nakagawara A, Arima-Nakagawara M, Scavarda NJ, Azar CC, Cantor AB, Brodeur GM. (1993). *N Engl J Med* **328**: 847–854.
- Nishihira J, Ishibashi T, Fukushima T, Sun B, Sato Y, Todo S. (2003). *Ann NY Acad Sci* **995**: 171–182.
- Ogawa H, Nishihira J, Sato Y, Kondo M, Takahashi N, Oshima T *et al.* (2000). *Cytokine* **12**: 309–314.
- Park M, Dean M, Cooper CS, Schmidt M, O'Brien SJ, Blair DG *et al.* (1986). *Cell* **45**: 895–904.
- Pritchard J, Hickman JA. (1994). *Lancet* **344**: 869–870.
- Ren Y, Chan HM, Li Z, Lin C, Nicholls J, Chen CF *et al.* (2004). *Oncogene* **23**: 4146–4154.
- Ren Y, Law S, Huang X, Lee PY, Li Z, Bacher M *et al.* (2005). *Ann Surg* **242**: 55–63.
- Ren Y, Tsui HT, Poon RT, Ng IO, Li Z, Chen Y *et al.* (2003a). *Int J Cancer* **107**: 22–29.
- Ren Y, Poon RT, Tsui HT, Chen WH, Li Z, Lau C *et al.* (2003b). *Clin Cancer Res* **9**: 5996–6001.
- Sasaki Y, Kasuya K, Nishihira J, Magami Y, Tsuchida A, Aoki T *et al.* (2002). *Int J Mol Med* **10**: 579–583.
- Seeger RC, Brodeur GM, Sather H, Dalton A, Siegel SE, Wong KY *et al.* (1985). *N Engl J Med* **313**: 1111–1116.
- Seeger RC, Wada R, Brodeur GM, Moss TJ, Bjork RL, Sousa L *et al.* (1988). *Prog Clin Biol Res* **271**: 41–49.
- Shimizu T, Abe R, Nakamura H, Ohkawara A, Suzuki M, Nishihira J. (1999). *Biochem Biophys Res Commun* **264**: 751–758.
- Tang XX, Robinson ME, Riceberg JS, Kim DY, Kung B, Titus TB *et al.* (2004). *Clin Cancer Res* **10**: 5837–5844.
- Tang XX, Zhao H, Robinson ME, Cohen B, Cnaan A, London W *et al.* (2000). *Proc Natl Acad Sci USA* **97**: 10936–10941.
- Tomiyasu M, Yoshino I, Suemitsu R, Okamoto T, Sugimachi K. (2000). *Clin Cancer Res* **8**: 3755–3760.
- Xie K. (2001). *Cytokine Growth Factor Rev* **12**: 375–391.
- Yang Y, Degranpre P, Kharfi A, Akoum A. (2000). *J Clin Endocrinol Metab* **85**: 4721–4727.